Structural Engineering and Mechanics, Vol. 9, No. 5 (2000) 505-518
DOI: http://dx.doi.org/10.12989/sem.2000.9.5.505

Retrofitting by adhesive bonding steel plates to the sides of R.C. beams. Part 2: Debonding of plates due to shear and design rules

Deric. J. Oehlers† and Ninh T. Nguyen‡

Department of Civil and Environmental Engineering, University of Adelaide, SA 5050, Australia

Mark A. Bradford‡†

School of Civil Engineering, University of New South Wales, Australia

Abstract. A major cause of premature debonding of tension face plates is shear peeling (Jones *et al.* 1988, Swamy *et al.* 1989, Ziraba *et al.* 1994, Zhang *et al.* 1995), that is debonding at the plate ends that is associated with the formation of shear diagonal cracks that are caused by the action of vertical shear forces. It is shown in this paper how side plated beams are less prone to shear peeling than tension face plated beams, as the side plate automatically increases the resistance of the reinforced concrete beam to shear peeling. Tests are used to determine the increase in the shear peeling resistance that the side plates provide, and also the effect of vertical shear forces on the pure flexural peeling strength that was determined in the companion paper. Design rules are then developed to prevent premature debonding of the plate ends due to peeling and they are applied to the strengthening and stiffening of continuous reinforced concrete beams. It is shown how these design rules for side plated beams can be adapted to allow for propped and unpropped construction and the time effects of creep and shrinkage, and how side plates can be used in conjunction with tension face plates.

Key words: retrofitting; rehabilitation; adhesive bonding; plating; reinforced concrete; shear peeling.

1. Introduction

Tests on tension face plated beams (Oehlers 1992) have shown that vertical shear forces can induce debonding of the tension face plate, that is shear peeling, and that the vertical shear forces reduce the flexural peeling resistance derived in the companion paper (Oehlers, Nguyen and Bradford 1998a). The reduction in the flexural peeling resistance of tension face plated beams is shown as the failure envelope A-B-C-D in Fig. 1 which has been quantified in terms of: M_{pure}=pure flexural peeling capacity which is the moment to cause the plate to debond when the plate-end is in a constant moment region as in Fig. 1(b); V_{pure}=pure shear peeling capacity which is the shear load

† Senior Lecturer
‡ Former Research Fellow
‡† Professor

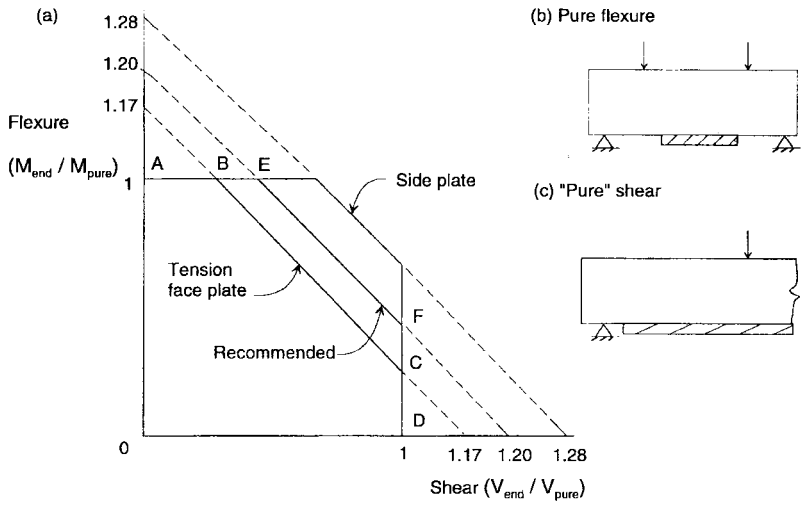

Fig. 1 Failure envelopes for tension face plated beams

to cause debonding when the plate is terminated adjacent to the support of a simply supported beam as in Fig. 1(c); M_{end}=moment at the plate-end applied after plating; and V_{end}=total applied vertical shear load at the plate-end. A similar approach has been applied in this paper to side plated beams.

The pure shear peeling resistance of side plated beams and the interaction between flexural peeling and shear peeling is determined experimentally, and the results used to develop failure envelopes to prevent debonding of side plated beams. The research is then presented in the form of design rules for both side plated beams and tension face plated beams and it is shown how these rules can cope with creep and shrinkage. An analysis procedure is then presented and applied to plating a continuous reinforced concrete beam: to increase the strength using propped and unpropped construction; to increase the strength for long term loads; to increase the stiffness at serviceability loads; and to illustrate mixed construction consisting of a combination of side plates and tension face plates.

2. Shear peeling

2.1. Experimental work

Details of the shear peeling tests and specimens are given in Fig. 2 and Table 1 where t_{sp}= thickness of side plate, h_p=height of plate and V_{end}=shear load at which debonding occurred. Each shear span of the beam in Fig. 2(a) was tested and the individual tests are listed in Table 1 where the debonding of each plate in a shear span was treated as an individual test; for example in column 1, tests 2n1N and 2n1S refer to beam 2n, shear span 1 of the two shear spans, and the plate on either the north side N or the south side S. The plate was terminated over a support, as shown in Fig. 2(a), so that the plate-end was subjected to pure shear. Some shear spans had the stirrups shown in Fig. 2(b) and others did not have stirrups as indicated in column (4) in Table 1. The concrete properties consisted of a compressive cylinder strength f_c=58 N/mm^2, Young's modulus E_c =37 kN/mm^2 and Brazilian tensile strength f_b=4.64 N/mm^2. The material properties of the plate and

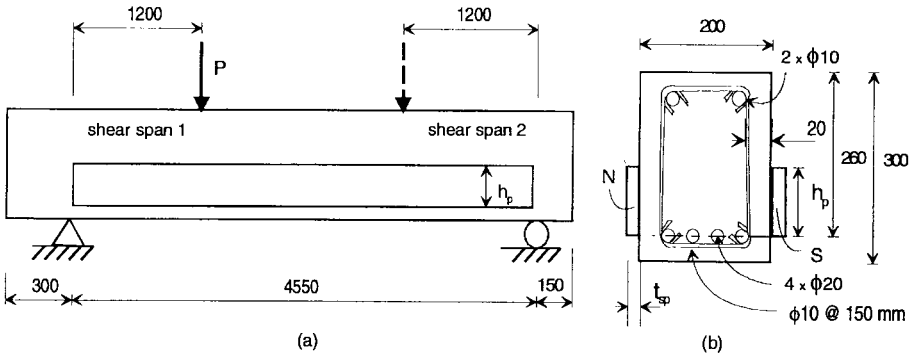

Fig. 2 Test rig and specimen for shear peeling

Table 1 Shear peeling tests

Tests	t_{sp}	h_p	Stirrups	V_{end}	τ
	(mm)	(mm)		(kN)	(N/mm^2)
(1)	(2)	(3)	(4)	(5)	(6)
2n1N	5	65	no	103.0	1.07
2n1S	5	65	no	103.0	1.07
2n2N	5	65	yes	125.9	1.31
2n2S	5	65	yes	128.1	1.33
2n3N	8	65	no	108.6	1.63
2n3S	8	65	no	105.8	1.59
2n4N	8	65	yes	126.5	1.90
2n4S	8	65	yes	126.5	1.90
2a1	0	0	no	85.1*	0
2a2	0	0	no	85.1*	0
2c	8	210	yes	176.9**	0.90

*V_{uc}. **had not debonded

reinforcing bars are given in the companion paper. Beam 2a in Table 1 was tested to determine the shear strength of the unplated beam without stirrups V_{uc} and Beam 2c did not fail due to shear peeling as the test was stopped at a shear load of 177 kN when the plate started to yield due to flexure. Full details are given elsewhere (Nguyen and Oehlers 1997a).

Strain gauges were placed along the length of the plate and at the mid-height of the plate to detect the occurrence of debonding. A typical variation in these longitudinal strains is shown in Fig. 3, where strain gauge 13 was placed below the applied load P in Fig. 2(a) and gauge 16 was placed 60 mm from the plate-end and with the other gauges uniformly spaced. It can be seen that gauge 16 indicated debonding adjacent to the plate-end at about 140 kN. However, the system remained stable until rapid crack propagation occurred at the load at which the remaining three strain gauges reduced rapidly. Shear peeling of side plated beams, as compared to flexural peeling in the companion paper, is a very rapid failure mechanism with virtually no warning, as occurred with tension face plated beams (Oehlers and Moran 1990). An example of debonding due to shear peeling is shown in Fig. 4 where the applied loads at which the cracks occurred are marked

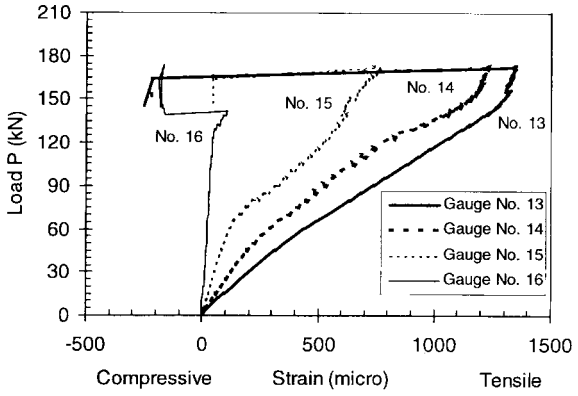

Fig. 3 Strains in test 2N2

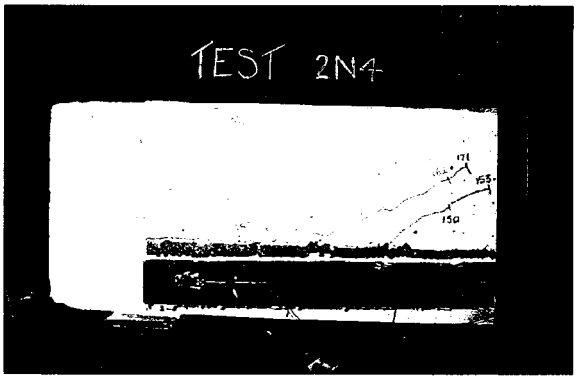

Fig. 4 Pure shear peeling (test 2N4)

adjacent to the crack. In this beam, the plates debonded at an applied load of 171 kN. However, it can be seen that diagonal cracking which occurred at 150 kN, preceded debonding and it is also worth noting that debonding occurred at 60% of the estimated shear capacity of the beam which confirms previous research (Oehlers 1992) that showed that the shear strength of a beam with stirrups does not affect debonding.

The shear loads at which debonding occurred are listed in column 5 of Table 1. Comparing test 2n3 without stirrups with test 2n4 with stirrups shows that the stirrups have increased the shear peeling resistance by 18% even though the stirrups in these beams would, in theory, have increased the shear strength of the beam by 150%. Hence shear peeling of 2n4 with stirrups occurred well before the vertical shear strength of the beam and, therefore, shear peeling can be said to be independent of the stirrups. This was shown to occur with tension face plated beams (Oehlers 1992) and, as with tension face plated beams, it will be assumed that the shear peeling strength of side plated beams is the shear strength of the side plated beams without stirrups. It is also worth noting that the shear stresses at debonding, τ in column (6), as derived from the well known VAy/Ib or VQ/It formula are much less than the tensile strength of the concrete and, hence, this equation should not be used to prevent debonding.

2.2. Shear peeling resistance

The pure shear peeling strength V_{pure}, as with the shear strength of unplated beams without stirrups V_{uc} (Zsutty 1968), is a very complex problem and, therefore, the effect of side plates will be determined empirically. It has been shown experimentally (Oehlers and Moran 1990, Oehlers 1992) that shear peeling of tension face plated beams occurs after the formation of diagonal cracks as shown in Fig. 5(a). These tests also showed that the shear strength of the these tension face plated beams without stirrups, $V_{uc,tfp}$, can be used for the shear peeling resistance V_{pure}. Furthermore, it was suggested that as the tension face plate forces the diagonal crack to occur at the plate-end where $V_{uc,tfp} > V_{uc}$ and, hence, a conservative approach would be to assume $V_{pure} = V_{uc}$ as V_{uc} is given in most national standards.

In further research into shear peeling of tension face plates (Oehlers, Ali and Luo 1998b, Luo 1993), plates were bonded to the sides of the beam as shown in Fig. 5(b), and it was found that when plates are bonded to both sides of the beam as in Fig. 2b, then the increase in the shear

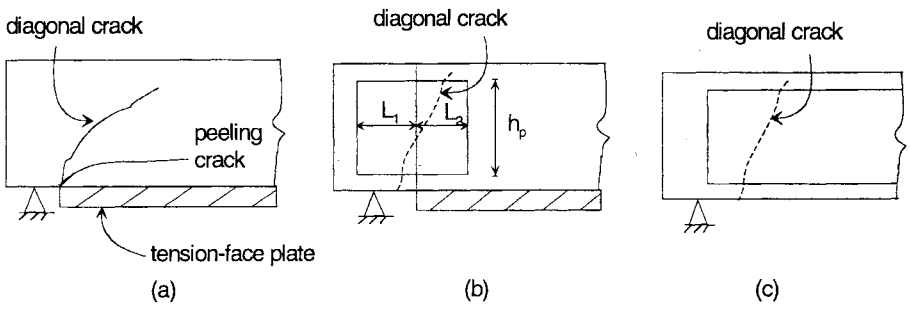

Fig. 5 Shear peeling resistance

peeling resistance ΔV_{pure} depends on the bond strength, and is given by

$$\Delta V_{pure}=0.12L_{\min}h_p f_b \tag{1a}$$

where $L_{\min}$=smaller of the two lengths L in Fig. 5(b). Eq. (1a) has the following upper limit that depends on the shear strength of the plate

$$\Delta V_{pure} \leq 0.30h_p t_{sp} f_{yp} \tag{1b}$$

where f_{yp}=yield strength of the side plate. Furthermore, the following geometric restriction was applied

$$0.80h_p \leq L_{\min} \leq 2h_p \tag{1c}$$

in order to limit the aspect ratio of the plates to those used in the tests.

In the tension face plated beams in Figs. 5(a) and 5(b), diagonal cracking always initiates adjacent to the end of the tension face plate where the beam is weakest in shear. The problem with the side plated beam in Fig. 5(c), as compared to the tension face plated beams in Figs. 5(a) and 5(b), is that the position at which the diagonal crack initiates is not defined. To overcome this, we will use the upper limit in Eq. (1c). Applying this upper limit to Eqs. (1a) and 1b gives the following increase in the shear peeling strength due to side plates, which is applicable to beams with only side plates and when the beam is plated on both sides.

$$\Delta V_{osp}=0.24h_p^2 f_b \tag{2a}$$

$$\Delta V_{osp} \leq 0.30h_p t_{sp} f_{yp} \tag{2b}$$

Tests 2n4 in Table 1 were 18 kN stronger than Tests 2a which measured V_{uc} directly, whereas, Eq. (2a) predicts an increase in the shear peeling resistance of 5 kN. As discussed previously, part of this discrepancy could be due to the plate causing the diagonal crack to move to the supports, so that Tests 2a would be an under-estimation of $V_{uc,tfp}$. Test 2c was at least 50 kN stronger than Tests 2n4, whereas, Eq. (2a) predicts an increase of 44 kN. Both comparisons suggest that Eq. (2) is conservative and can be used in design. It is also worth noting that tests 2n2 and tests 2n4 had virtually the same strength, even though the area of the plate in the latter was 60% greater. However, because the depth of the plate, and hence the bonded area, was the same in both tests, they failed at the same strength as predicted by Eq. (2a).

In conclusion, the shear peeling resistance of beams with only side plates $V_{pure,sp}$ is given by

$$V_{pure,sp}=V_{uc}+\Delta V_{osp} \tag{3}$$

3. Interaction between shear and flexural peeling

Having quantified the peeling resistance when there is pure flexure, M_{pure} in Part 1, and the peeling resistance when there is pure shear, $V_{pure,sp}$ in Eq. (3), the interaction between shear and flexural peeling is now determined experimentally.

3.1. Experimental work

Details of the specimens and test rig are given in Fig. 6 and Table 2 where L_{end}=distance of the plate-end from the support, M_{end}=moment at plate-end at which the plate debonded and ε_u= maximum strain in the plate at debonding. The moment/shear-force ratio at the plate-end was varied by changing the distance L_{end} in Fig. 6(a) and these distances are listed in column (2) in Table 2. Each plate was treated as an individual test as shown in column (1). The concrete material properties were E_c=40.4 kN/mm^2, f_b=4.49 N/mm^2 and f_c=52.4 N/mm^2, the properties of the steel components are given in the companion paper, and full details of the tests are given elsewhere (Nguyen and Oehlers 1997b). As with the flexural peeling tests in the companion paper and the shear peeling tests previously described in this paper, the plates were strain gauged to detect the onset of debonding.

The shear load at debonding V_{end} and the moment at the plate-end at debonding M_{end} are listed in columns (3) and (4) in Table 2. The maximum shear stess τ and strain in the plate ε_u at debonding, which occurred in the gauge under the applied load, are listed in columns (5) and (6) in Table 2. It can be seen that there is a wide range in ε_u and τ at debonding and, hence, these parameters cannot be used to predict debonding.

3.2. Failure envelopes

For the shear-flexural peeling tests in Table 2, the theoretical mean pure flexural peeling capacity $M_{pure,mn}$ can be derived from Eq. (17) of the companion paper, whereas, the pure shear peeling capacity $V_{pure,sp}$ is given by tests 2n4 in Table 1, as these beams had the same stirrups and plates as those used in Table 2. Therefore, the experimental results V_{end} and M_{end} in Table 2 can be non-dimensionalised by dividing by $M_{pure,mn}$ and $V_{pure,sp}$ as shown in Fig. (7); it can be seen that there is a strong interaction between these stress resultants.

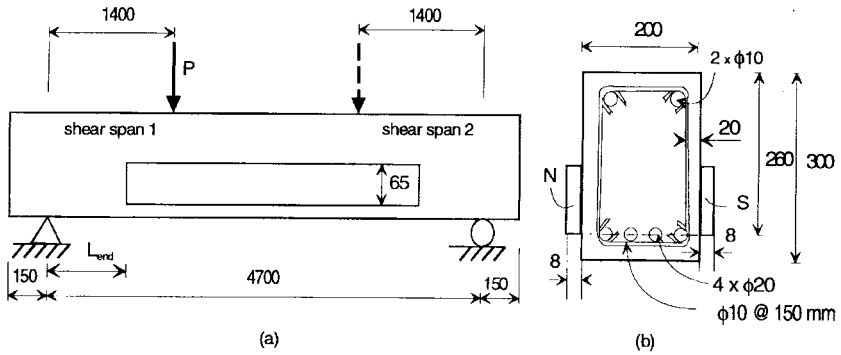

Fig. 6 Test rig and specimen for shear/flexure peeling

Table 2 Shear/flexure peeling tests

Tests	L_{end}	V_{end}	M_{end}	e_u	τ
	(mm)	(kN)	(kNm)	(10^{-6})	(N/mm^2)
(1)	(2)	(3)	(4)	(5)	(6)
3c1N	300	103.1	30.9	1241	1.52
3c1S	300	103.1	30.9	1243	1.52
3c2N	300	104.5	31.3	1245	1.54
3c2S	300	104.5	31.3	1272	1.54
3d1N	910	74.7	68.0	725	1.10
3d1S	910	72.6	66.1	773	1.07
3d2N	910	87.5	79.6	836	1.29
3d2S	910	76.9	70.0	710	1.14
3e1N	2740	40.3	110.3	890	0.60
3e1S	2740	36.2	99.3	980	0.53
3e2N	2395	42.1	100.9	979	0.62
3e2S	2395	28.6	68.6	770	0.42
3f1N	1200	65.2	78.3	831	0.96
3f1S	1200	52.0	62.4	709	0.77
3f2N	1200	55.7	66.9	718	0.82
3f2S	1200	55.7	66.9	812	0.82

A linear regression analysis of the results in Fig. 7 (Nguyen and Oehlers 1997b) gave

$$\frac{M_{end}}{M_{pure,mn}}+1.15\frac{V_{end}}{V_{pure,sp}}=1.36 \tag{4}$$

which has a standard deviation is 0.143, and in which the characteristic value of the equation at the 5% confidence limit can be determined by replacing the coefficient 1.36 with 1.11.

The failure envelope for tension face plated beams, shown in Fig. 1, has a slope of–1. Applying

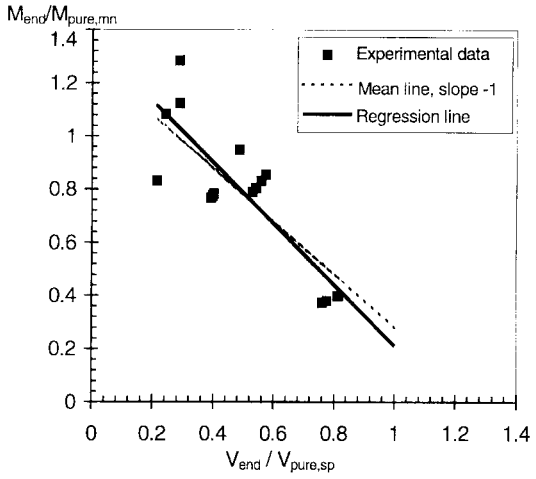

Fig. 7 Interaction between shear and flexural peeling

the same procedure to side plated beams, the line with a slope of−1 and which passes through the mean of the results in Fig. 7 is given by

$$\frac{M_{end}}{M_{pure,mn}}+\frac{V_{end}}{V_{pure,sp}}=1.28 \tag{5}$$

which has a standard deviation of 0.147 and which is only slightly larger than the standard deviation from the linear regression approach of 0.143. It would appear that the form of failure envelope developed for tension face plated beams can also be used for side plated beams with very little loss of accuracy. Eq. (5) is compared with the failure envelope for tension face plates in Fig. 1. The characteristic value for Eq. (5) can be obtained by replacing the coefficient 1.28 with 1.02.

4. Design rules

4.1. Recommendations

Design rules should be developed according to national procedures. However, the following recommendations for the failure envelope in Fig. 1 are suggested for both side plated beams and tension face plated beams.

- M_{pure}= the characteristic pure flexural peeling capacity $M_{pure,ch}$
- $V_{pure}=f(V_{uc})$ where V_{uc} is either determined experimentally or the values in national standards are used as these are usually characteristic or lower bound values
- The mean value for the axis intercepts is used, as the scatter has already been allowed for by using the characteristic values for M_{pure} and V_{uc}
- The individual intercept values of 1.17 and 1.28 in Fig. 1 can be used in design. Alternatively a value close to the intercept value for tension face plated beams, such as 1.20 as shown in Fig.1, is recommended, as the testing program for tension face plated members was much more extensive than that for side plates.

4.2. General design rules

The recommended design failure envelope, shown in Fig. 1, is defined by

$$\frac{M_{end}}{M_{pure}}+\frac{V_{end}}{V_{pure}}=K\le 1.20 \tag{6a}$$

$$M_{end}\le M_{pure} \tag{6b}$$

$$V_{end}\le V_{pure} \tag{6c}$$

where Eq. (6a) defines the sloping part of the failure envelope E-F in Fig. 1(a), Eq. (6b) defines the horizontal part of the failure envelope A-E, and where Eq. (6b) defines the vertical part of the failure envelope F-D, and where M_{end}=moment applied to the beam at the plate-end after plating, whereas, V_{end}=total vertical shear force applied at the plate-end.

For side plated beams

$$M_{pure,sp}=\frac{0.805f_b(EI)_{cmp}}{E_p(0.0185h_{p,cmp}+0.185t_{sp})} \tag{7}$$

$$V_{pure,sp}=V_{uc}+0.24h_p^2 f_b \tag{8a}$$

in which the parameter

$$0.24h_p^2 f_b \le 0.30h_p t_{sp} f_{yp} \tag{8b}$$

where $(EI)_{cmp}$=flexural rigidity of the cracked plated section, E_p=Young's modulus of plate, and $h_{p,cmp}$ =distance between the centroid of the cracked plated section and the centroid of the plate.

For tension face plated beams

$$M_{pure,\,tfp}=\frac{f_b(EI)_{cmp}}{0.901E_p t_{tfp}} \tag{9}$$

$$V_{pure,\,tfp}=V_{uc}+0.12L_{min}h_p f_b \tag{10a}$$

in which the parameter

$$0.12L_{min}h_p f_b \le 0.30h_p t_{sp} f_{yp} \tag{10b}$$

and

$$0.80h_p \le L_{min} \le 2h_p \tag{10c}$$

where t_{tfp} = thickness of the tension face plate.

4.3. Time effects for side plated beams

The simplest way of allowing for the effects of creep is to use the long term flexural rigidities in Eqs. (7) and (9). However, if it is necessary to differentiate between creep and shrinkage and long and short terms loads, then a more suitable procedure is to write Eq. (6a) in the following form

$$\frac{\chi_{short}}{\chi_{pure}}+\frac{\chi_{creep}}{\chi_{pure}}+\frac{\chi_{shrink}}{\chi_{pure}}+\frac{V_{end}}{V_{pure}}=K \le 1.20 \tag{11}$$

where from Eq. (7), the denominator χ_{pure} in Eq. (11) is given by

$$\chi_{pure,sp}=\frac{0.805f_b}{E_p(0.0185h_{p,cmp}+0.185t_{sp})} \tag{12}$$

and where χ_{short} = curvature induced in the cracked plated beam through short term loads, χ_{creep} = increase in curvature due to creep and χ_{shrink} = increase in curvature due to shrinkage. The same arrangement can be applied to tension face plated beams (Oehlers 1995).

5. Analysis procedure

The general analysis procedure is illustrated in Fig. 8 for a half span of a continuous beam. Let us assume that the engineer has chosen the cross-sectional size and the vertical position of the side plates to satisfy some design requirement which could be for strength or stiffness. The problem is to determine where the plate-end can be terminated in order to ensure that they do not debond prematurely. It will be assumed that shear stress debonding which occurs between the plate-ends

will be checked independently using the well known VAy/Ib or VQ/It formula; experience has shown that this failure mode seldom controls the design. The plate can be either started at a support and extended to the right as shown in Fig. 8(a) or it can be started at mid-span and extended to the left or a combination of these procedures can be used.

The first step is to determine the distribution of the applied moment to design for. This is shown as M_{end} in Fig. 8(b). It must be emphasised that this is the moment distribution applied to the beam after plating, as it is the curvature after plating that induces flexural peeling. Therefore, if the beam is propped prior to plating, then M_{end} is the total moment applied to the beam. In contrast, if the beam is unpropped prior to plating then M_{end} is the additional moment after plating which may consist of just the live load. For complex loading conditions, M_{end} in Fig. 8(b) may consist of a family of moment envelopes. Also plotted in Fig. 8(b) are the pure flexural peeling capacitiesM_{pure} which are properties of the cross-section of the beam and which may vary along the length of the beam. It is assumed in this example that there are two values, one for the hogging region,$M_{pure,hog}$ and the other for the sagging region, $M_{pure,sag}$. In order to ensure that Eq. (6b) is satisfied, the plate-ends must not be terminated within the region marked with arrows in Fig. 8(b), as within these arrowed regions $M_{end} > M_{pure}$.

The next step, shown in Fig. 8(c), is to determine the distribution or envelopes of applied vertical shear V_{end}, where V_{end} is the total vertical shear load as shear peeling depends on the formation of

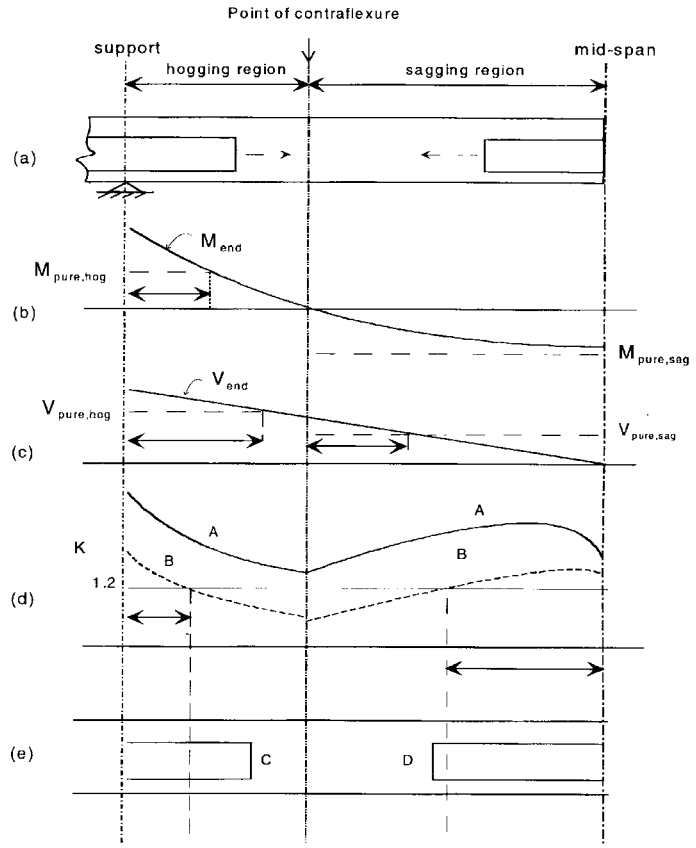

Fig. 8 General analysis procedure

diagonal shear cracks. This is compared with the pure shear peeling capacity V_{pure} which may vary along the length of the beam as it depends on the distribution of the tensile reinforcing bars. In this example, two values of V_{pure} are shown, one for the hogging region and the other for the sagging region. In order to satisfy Eq. (6c), the plates must not be terminated within the arrowed regions where $V_{end} > V_{pure}$.

The third design criterion given by Eq. (6a) is checked in Fig. 8(d). The magnitude of K in Eq. (6a) is determined at different points along the beam and the results plotted as shown. The variation of K is then compared with the value to cause debonding which in Eq. (6a) is 1.20. It can be seen if the values of K given by lines A in Fig. 8(d) apply, then the beam cannot be plated. However, if the variation given by lines B apply, then the plates must not be terminated within the arrowed region where $K > 1.20$.

The results of the analysis are shown in Fig. 8(e). It can be seen in Fig. 8(e) that the plate extending from the support can be terminated at point C, as point C lies outside the arrowed regions in the hogging region of Figs. 8(b), (c) and (d). Whereas, the plate extended from mid-span can also be terminated at point D which lies outside the arrowed regions in the sagging region.

6. Application

6.1. General

Let us consider an interior span of a continuous reinforced concrete beam with a span of 18 m and which was originally designed for a load of 50 kN/m. The material properties consist of $f_c = 30$ N/mm^2, $E_c = 30$ kN/mm^2, $f_b = 3$ N/mm^2, $E_r = E_p = 210$ kN/mm^2, long term $E_c = 15$ kN/mm^2, $f_{yp} = 350$ N/mm^2, $V_{uc,sag} = 250$ kN and $V_{uc,hog} = 300$ kN. The following analyses will only deal with the sloping part of the failure envelope, that is line E-F in Fig. 1 and Eq. (6a), and we will only deal with debonding due to peeling of the plate-ends.

6.2. Case 1: Rectangular beam with side plates and propped construction

In order to illustrate the effect of side plating, we will consider a beam that is rectangular throughout although these occur rarely in practice. The cross-section of the beam in the positive or sagging region is shown in Fig. 9(a) and that in the hogging region in Fig. 9(b). Let us assume that it is necessary to increase the design load from 50 kN/m to 75 kN/m and that propped construction is used so that all of the stress resultants are resisted by the action of the composite plated beam. Hence at the ultimate load, the continuous beam has to resist a maximum hogging moment $M_{max,hog} = -2025$ kNm, a maximum sagging moment $M_{max,sag} = 1013$ kNm and a maximum shear load $V_{max} = 675$ kN.

The plate depths of 650 mm in Figs. 9(a) and (b) have been chosen so that they substantially increase the pure shear peeling capacity (from Eq. (8), $\Delta V_{pure} = 304$ kN when $t_{sp} > 4.5$ mm) so it will be assumed that this dimension is unchanged and instead the plate thicknesses have been varied, and the results of applying Eq. (6a) are shown in Fig. 10. Let us consider the 3 mm plate. The results show that peeling will not occur if the plates are terminated within the region B-C as shown in the diagram of the plated beam. However if the plate thickness is increased to 5 mm, the region within which the plate can be terminated increases to A-C, whereas, the 10 mm and 15 mm plates can be terminated anywhere within the region A-A. Hence for this cross-section of beam,

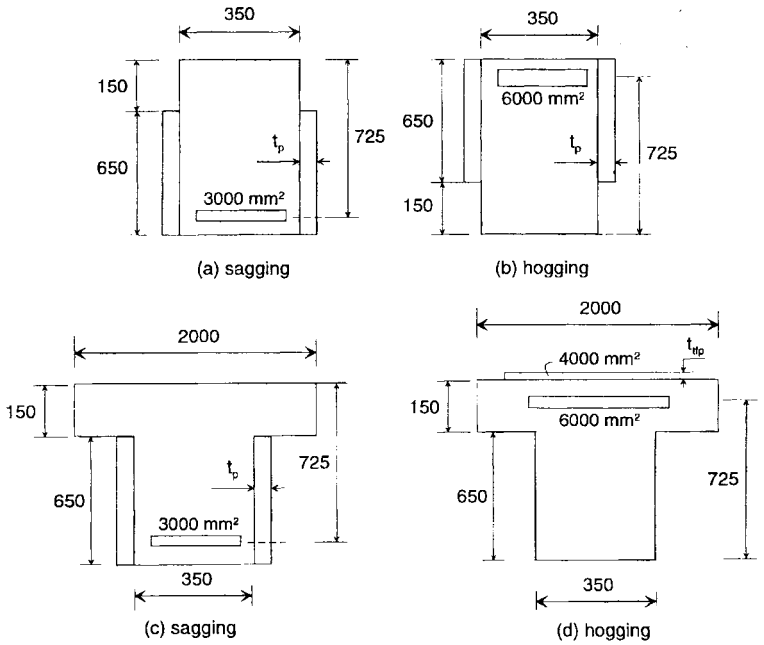

Fig. 9 Sectional properties of continuous beam

increasing the thickness of the plate inhibits debonding. This is because for this cross-section as t_{sp} increases, $h_{p,cmp}$ reduces causing the denominator in Eq. (7) to remain fairly constant, whereas $(EI)_{cmp}$ in the numerator substantially increases with increasing t_{sp} causing the pure flexural peeling capacity to increase which is in contrast to the beams tested in the companion paper.

A rigid plastic analysis shows that in order to increase the flexural capacity by 50% it is necessary to add 3 mm side plates to the sagging region and 10 mm side plates to the hogging region which according to Fig. 10 can be easily accommodated.

6.3. Case 2: T-beam with side and tension-face plates

Now let us consider a more realistic situation of a continuous composite T-beam with the

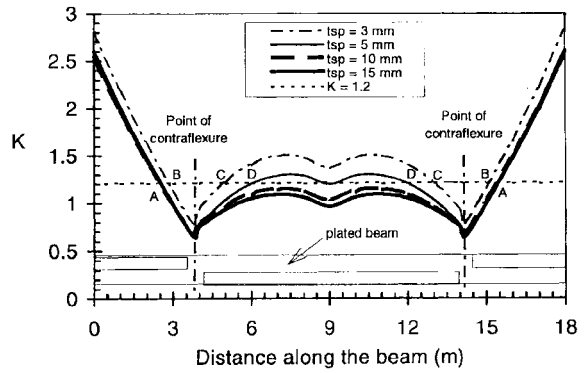

Fig. 10 Rectangular side-plated beam

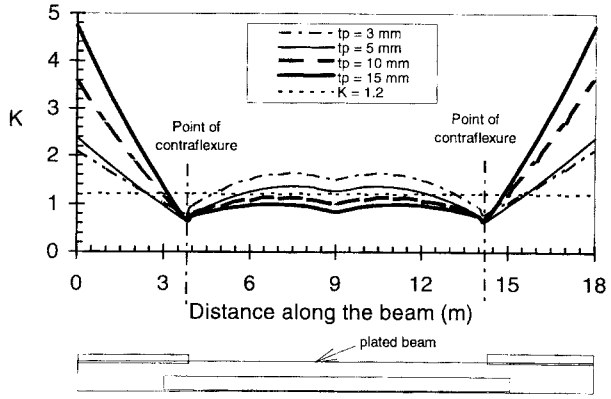

Fig. 11 Mixed construction

sectional properties shown in Figs. 9(c) and (d). The sagging region is plated on its sides and the hogging region has a tension face plate of constant area of 4000 mm^2. It can be seen in the diagram within Fig. 11 that the side-plate has been terminated beyond the end of the tension face plate so that the side-plate increases the pure shear peeling capacity at the end of the tension face plate. The results in Fig. 11 show that this beam can be plated for a wide variety of plate thicknesses. It is also of interest to note that the results show that debonding can be inhibited in the sagging region where there are side-plate by increasing the plate thickness, whereas, in the hogging region where there is a tension face plate the plate thickness has to be reduced to inhibit debonding.

6.4. Case 3: Side plated T-beam in sagging region

The versatility of this design procedure is illustrated in Fig. 12 for side plated beams in the sagging region with the section in Fig. 9(c) with a 5 mm plate. Analyses (a) to (c) in Fig. 12 are ultimate strength analyses that allow for the effects of time (creep and shrinkage) and forms of construction (propped and unpropped construction). Whereas analysis (d) requires the plating to only resist serviceability loads.

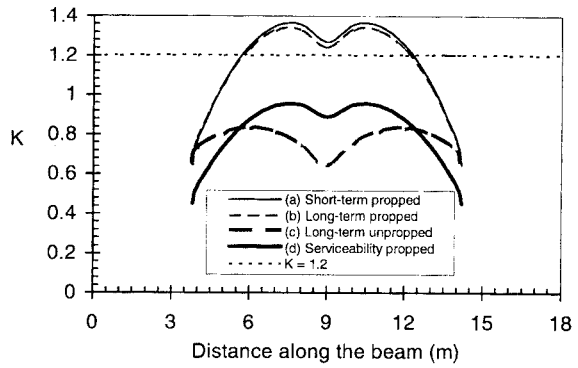

Fig. 12 Side-plated sagging region

7. Conclusions

A design procedure has been developed for adhesive bonding steel plates to the sides of reinforced concrete beams that ensures that the plate-ends do not debond prematurely. The procedure has been developed from mathematical models and from 39 additional beam tests.

Acknowledgements

This work forms part of an ongoing research project between the Universities of New South Wales and Adelaide that is funded by the Australian Research Council.

References

Jones, R., Swamy, R.N. and Charif, A. (1988), "Plate separation and anchoragte of reinforced concrete beams strengthened by epoxy-bonded steel plates", *The Structural Engineer*, **66**(5), 85-94.

Nguyen, N.T. and Oehlers, D.J. (1997a), "Experimental investigation of side-plated beams subjected to both flexural peeling and shear peeling", Dept. of Civil and Environmental Engng., University of Adelaide, Research Report R 142, April.

Nguyen, N.T. and Oehlers, D.J. (1997b). "Interaction curves for flexural and shear peeling of side-plated glued beams", Dept. of Civil and Environmental Engng., University of Adelaide, Research Report R 152, April.

Oehlers, D.J. (1992), "Reinforced concrete beams with plates glued to their soffits", *Journal of Structural Engineering, ASCE*, **118**(8), Aug. 2023-2038

Oehlers, D.J. (1995), "Rules for bonding steel plates to existing reinforced concrete slabs", *Australian Civil Engineering Transactions*, **CE37**(1), Feb.,15-20.

Oehlers, D.J. and Moran, J.P. (1990), "Premature failure of externally plated reinforced concrete beams", *Journal of Structural Engineering, ASCE*, **116**(4), 978-995, April.

Oehlers, D.J., Nguyen, N.T. and Bradford, M.A. (2000), "Retrofitting by adhesive bonding steel plates to the sides of R.C. beams. Part 1: Debonding of plates due to flexure", *Structural Engineering and Mechanics, An Int'l Journal*, **9**(5), 491-504.

Oehlers, D.J., Mohamed Ali, M.S. and Lou, W. (1998b), "Upgrading continuous reinforced concrete beams by gluing steel plates to their tension faces", *Journal of Structural Engineering, ASCE,* Mar., **124**(3).

Swamy, R.N., Jones, R. and Charif, A. (1989), "The effect of external plate reinforcement on the strengthening of structurally damaged RC beams", *The Structural Engineer*, **67**(3), 45-56.

Zhang, S., Raoof, M. and Wood, L.A. (1995), "Prediction of peeling failure of reinforced concrete beams with externally bonded steel plates", *Proc. Institution of Civil Engineers, Structures and Buildings*, **110**(aug), 257-268.

Ziraba, Y.N., Baluch, M.H. and Basunbul, I.A. *et al.* (1994), "Guidelines toward the design of reinforced concrete beams with external plates", *ACI Structural Journal,* **91**(6), 639-646.